Allergologia et immunopathologia
Sociedad Española de Inmunología Clínica, Alergología y Asma Pediátrica
www.all-imm.com

ORIGINAL ARTICLE

OPEN ACCESS

Peucedanum japonicum Thunberg root extract inhibits atopic dermatitis-like skin symptoms

Jang Hoon Kim[a], Kyung-Sook Han[a], Eun Seo Kang[b,c], Ji Hyeon Park[c], Byoung Ok Cho[c]*, Jae Ho Choi[d,e]*

[a]*Department of Herbal Crop Research, National Institute of Horticultural & Herbal Science, RDA, Eumsung, Republic of Korea*
[b]*Department of Environmental Life and Food Sciences, Jeonju University, Jeonju-si, Jeollabuk-do, Republic of Korea*
[c]*Institute of Health Science, Jeonju University, Jeonju-si, Jeollabuk-do, Republic of Korea*
[d]*Inflamm-Aging Translational Research Center, Ajou University Medical Center, Suwon, Republic of Korea*
[e]*Department of Hematology-Oncology, Ajou University School of Medicine, Suwon, Republic of Korea*

Received 27 April 2025; Accepted 11 June 2025
Available online 1 September 2025

KEYWORDS
Peucedanum japonicum Thunberg root extract;
atopic dermatitis-like skin symptoms;
inflammation;
NF-κB;
therapeutic agent

Abstract
Peucedanum japonicum Thunberg is a perennial herbaceous plant of the genus *Peucedanum* that belongs to the Apiaceae family and is effective in improving inflammation, gout, and dizziness. However, the skin pruritus improvement effect and mechanism of action of *Peucedanum japonicum* Thunberg root extract (PJRE) have not yet been reported. We investigated the effects of PJRE on the regulation of pruritus and inflammatory responses in compound 48/80 (C48/80)-treated mice, phorbol 12-myristate 13-acetate (PMA)/A23187-induced human skin mast cells, and LPS-stimulated mouse macrophages. PJRE administration significantly inhibited scratching behavior, skin inflammatory cells, and mast cell infiltration in mice increased by C48/80. PJRE treatment also reduced the PMA/A23187-activated secretion of histamine, inflammatory cytokines, and interleukins via NF-κB activation in HMC-1 cells. PJRE treatment reduced LPS-stimulated secretion of inflammatory cytokines and expression of iNOS and COX-2 through phosphorylation of NF-κB, Akt, ERK1/2, and p38 MAPK in Raw 264.7 cells. PJRE treatment increases HO-1 expression in a concentration-dependent manner via NRF2 nuclear translocation. These results suggest that PJRE has therapeutic potential for alleviating atopic dermatitis-like skin symptoms, which is likely mediated by NF-κB as a transcription factor and Akt, ERK1/2, and p38 MAPK as upstream signaling molecules.

***Corresponding authors**: Jae Ho Choi, Inflamm-Aging Translational Research Center and Department of Hematology-Oncology, Ajou University Medical Center, Suwon, Republic of Korea. *Email addresses*: chlkoala@ajou.ac.kr; jaehochoi78@gmail.com; Byoung Ok Cho, Institute of Health Science, Jeonju University, 303 Cheonjam-ro, Wansan-gu, Jeonju-si, Jeollabuk-do, Republic of Korea. *Email address*: enzyme21@jj.ac.kr

https://doi.org/10.15586/aei.v53i5.1399

Introduction

Atopic dermatitis (AD) is a multifactorial inflammatory skin condition characterized by a complex interplay between genetic predisposition,[1] immune dysregulation,[2] environmental factors,[3] and epidermal barrier dysfunction.[4,5] AD affects individuals of all ages worldwide, with a notable burden on the pediatric population. The pathogenesis of AD-like skin symptoms involves complex interactions between various cell types, including keratinocytes, mast cells, T cells, and dendritic cells, orchestrated by a network of cytokines, chemokines, and inflammatory mediators.[5]

The aberrant activation of immune cells and dysregulated inflammatory responses are central to the pathology of AD-like skin symptoms.[6] Mast cells, key effector cells in allergic and inflammatory reactions, play a pivotal role in the pathogenesis of AD-like skin symptoms through the release of histamine, cytokines, and other proinflammatory mediators upon activation. In addition, dysregulated T-cell responses skewed toward a Th2-dominant profile contribute to allergic inflammation and tissue damage in AD-like skin symptoms.[7]

Despite significant advances in understanding the pathophysiology of AD, the effective management of this diverse array of symptoms remains a clinical challenge. While topical corticosteroids and calcineurin inhibitors are commonly used to alleviate inflammation, their long-term use may lead to adverse effects, such as skin atrophy and increased susceptibility to infections.[8] Systemic immunomodulators, although effective, carry the risk of systemic toxicity and require careful monitoring.[9,10]

There is an increasing interest in exploring natural products as alternative or adjunctive therapies for AD-like skin symptoms.[11] With their complex mixtures of bioactive compounds, herbal medicines offer potential advantages, such as multitarget effects, fewer adverse effects, and better tolerability.[12] *Peucedanum japonicum* Thunberg root extract (PJRE), a traditional medicinal herb commonly used in East Asia, has demonstrated promising pharmacological activities, including anti-inflammatory,[13-20] antioxidant,[15] and wound-healing properties.[15] However, despite its pharmacological potential, the therapeutic effects of PJRE on AD-like skin symptoms have not yet been comprehensively investigated. Therefore, we hypothesized that PJRE may attenuate pruritus and inflammatory responses in atopic dermatitis (AD)-like conditions through its anti-inflammatory properties. Using a combination of mouse and cellular models, we elucidated the underlying mechanisms of PJRE action, focusing on its modulation of mast cell activation and macrophage stimulation. In this study, we evaluated the inhibitory effects of PJRE on AD-like skin symptoms and relevant signaling pathways in compound 48/80 (C48/80)-induced mice, phorbol 12-myristate 13-acetate (PMA)/A23187-activated HMC-1 cells, and LPS-stimulated Raw 264.7 cells.

Materials and Methods

Chemicals and materials

Ultra-high-performance liquid chromatography (UHPLC) was performed using an Agilent 1290 Infinity II system (Agilent, Santa Clara, CA, USA). High-performance liquid chromatography-grade (HPLC)-grade acetonitrile and water were purchased from Thermo Fisher Scientific (Waltham, MA, USA). Prednisolone (P6004), C48/80 (C2313), hematoxylin (H3136), eosin (E4009), toluidine blue (89640), Griess reagent (G1440), phorbol 12-myristate 13-acetate (PMA; P8139), lipopolysaccharides from *Escherichia coli* O111:B4 (LPS; L2630), and calcium ionophore A23187 (C7522) were purchased from Sigma-Aldrich (St. Louis, MO, USA). The Quanti-MAX™ WST-8 Cell Viability Assay Kit (QM1000) and WestGlow™ FEMTO Chemiluminescent substrate (BWF0200) were obtained from Biomax (Seoul, South Korea). Tin protoporphyrin IX dichloride (SnPP, 14325-05-4) was purchased from Thermo Fisher Scientific. NE-PER™ Nuclear and Cytoplasmic Extraction Reagent (78833), Alexa Fluor Plus 488 (A32723), and RIPA buffer were purchased from Invitrogen (Carlsbad, CA, USA). Bradford assay reagents were purchased from Bio-Rad Laboratories, Inc. (Hercules, CA, USA). SDS-PAGE loading buffer (5X) was purchased from Biosesang (Seongnam, Gyeonggi, South Korea).

Plant material

Peucedanum japonicum Thunberg roots were harvested in March 2021 from Geumodo Island, Yeosu, South Korea. A voucher specimen (PJR210330_1) was deposited in the herbarium of the Department of Herbal Crop Research, National Institute of Horticultural and Herbal Science, Rural Development Administration (RDA).

Extract and concentration

The roots of *P. japonicum* (10 g) were dried under ventilation at 45°C for 1 week and sonicated with 400 mL of ethanol (1 h × 3 times) at room temperature. Ethanol was filtered using paper filter and concentrated under reduced pressure to yield 2.7 g of the extract.

UHPLC profile of the chemical constitutes of Peucedanum japonicum *roots*

Ultra-high-performance liquid chromatography (UHPLC) analysis was performed using an Agilent 1290 Infinity II system with a diode array detector. The column for qualitative analysis was an Agilent poroshell 120 EC-C18 (1.9 μm, 2.1 × 50 mm) with a mobile phase consisting of a gradient of water and acetonitrile. The detection wavelength was set to 210 nm, and the column temperature was set to room temperature. The flow rate was 0.5 mL/min.[19]

Animals and experimental design

Four-week-old male ICR mice weighing 18 ± 2 g were obtained from Orient Bio Inc. (Seongnam, South Korea). The mice were housed under standard environmental conditions and fed a standard commercial diet and water ad libitum. The mice were maintained at a constant room temperature of 22 ± 2°C and humidity of 50–60% under a

12/12 h light/dark cycle. After 1 week of initial acclimatization, the animals were divided into five groups (N = 5 each): Group 1, normal control; Group 2, C48/80 only; Group 3, C48/80 + PJRE (100 mg/kg); Group 4, C48/80 + PJRE (200 mg/kg); and Group 5, C48/80 + prednisolone (10 mg/kg). To induce pruritus in Groups 2–5, 50 μg/site (0.1 mL) of C48/80 was subcutaneously injected into the left shoulder. Groups 1 and 2 were treated with saline, Groups 3 and 4 were treated with 100 and 200 mg/kg PJRE, respectively, and Group 5 was treated with 10 mg/kg prednisolone 60 min before the injection of C48/80. Thereafter, the scratching behavior was evaluated according to a method reported previously.[19] All animal procedures complied with the recommendations of the Guide for Care and Use of Laboratory Animals (National Research Council of Korea) and were approved by the Institutional Animal Care and Use Committee (Approval number: jjIACUC-20230602-2022-0502-A1) at Jeonju University.

Histopathological analysis

Dorsal skin sections from ICR mice injected with C48/80 were harvested. The tissues were fixed in 4% paraformaldehyde in phosphate-buffered saline (PBS, pH 7.4) for 24 h, washed in PBS for 24 h with five buffer changes, dehydrated by passage through a graded ethanol series (60–100%), cleared in xylene, and finally embedded in paraffin. Sections 5 μm thick were cut and stained with hematoxylin and eosin for the measurement of epidermal thickness, and with toluidine blue for mast cell quantification. Immunohistochemistry was performed using an anti-tryptase antibody to characterize the mast cell degranulation. Slides for immunohistochemistry were blocked with horse serum (Vector Laboratories, Burlingame, CA, USA) and incubated with an anti-tryptase antibody for 20 h. The slides were then incubated with ImmPRESS™ HRP reagent containing anti-mouse IgG (Vector Laboratories) for 30 min, followed by incubation for 25 min with AEC peroxidase substrate (Vector Laboratories). The slides were examined under a light microscope (Leica, Wetzlar, Germany).[19]

Cell culture

Human mast cells (HMC-1; Sigma-Aldrich) were cultured in Iscove's modified Dulbecco's medium (IMDM; Gibco, Thermo Fisher Scientific Korea, Seoul, South Korea) while RAW264.7 cells (TIB-71; ATCC, Manassas, VA, USA) were cultured in Dulbecco's Modified Eagle's medium (Gibco, Thermo Fisher Scientific Korea), both supplemented with 10% FBS and 1% penicillin/streptomycin at 37°C in a humidified incubator under an atmosphere of 5% CO_2.

Cell viability

Cell viability was evaluated by the MTT assay. Briefly, HMC-1 and RAW264.7 cells (1×10^4 cells/well) were seeded in 96-well plates and treated with PJRE (0–200 μg/mL). After 20 h, the cells were treated with Quanti-Max™, and the absorbance was measured at 450 nm after 4 h.

Nitric oxide assay

RAW 264.7 cells were cultured in 48-well plates for 24 h and pretreated with PJRE (0–100 μg/mL). After 1 h, the cells were incubated with lipopolysaccharide (LPS; 1 μg/mL) for 20 h. Aliquots of 100 μL of the supernatant and Griess reagent were added to 96-well plates, and the absorbance at 450 nm was measured after 15 min.

Enzyme-linked immunosorbent assay

HMC-1 and RAW 264.7 cells were cultured in 60-mm cell culture dishes for 24 h and pretreated with PJRE (0–100 μg/mL). After 1 h, the cells were stimulated with PMA (30 nM), A23187 (1 μM), or LPS (1 μg/mL) for 3 or 24 h. Culture supernatants were collected, and the concentrations of TNF-α, IL-1β, IL-6, IL-8, IL-31, histamine, and PGE_2 were measured. The concentrations for the enzyme-linked immunosorbent assay (ELISA) were determined according to the manufacturer's protocol. The ELISA kits used for TNF-α, IL-1β, IL-6, IL-8, IL-31, histamine, and PGE2 are listed in Supplementary Table 3. The NF-κB p65 Transcription Factor Assay Kit (ab133112) was obtained from Abcam (Waltham, MA, USA).

Protein extraction and western blotting

RAW264.7 cells were cultured in 60-mm cell culture dishes for 24 h and pretreated with PJRE (0–100 μg/mL). After 1 h, the cells were stimulated with LPS (1 μg/mL) for 30 min or 24 h. Proteins were extracted using RIPA buffer containing protease and phosphatase inhibitors. After quantification using the Bradford method, the proteins were separated by polyacrylamide gel electrophoresis (PAGE) at 100 V for 1 h. Proteins were transferred from the gels onto polyvinylidene difluoride (PVDF) membranes at 100 V for 1 h, and the membranes were then incubated overnight at 4°C. After washing three times with TBS/T solution for 10 min each, the membranes were incubated in 5% skim milk with mouse or rabbit HRP-conjugated secondary antibody for 2 h at room temperature. The primary and secondary antibodies used are listed in Tables S1 and S2, respectively. The membranes were washed three times with TBS/T solution for 10 min each and imaged with an imaging system (Alliance version 15.11; Uvitec, Cambridge, UK) using EZ-Western Lumi Pico Alpha reagent. Band densities were analyzed using the ImageJ software (National Institutes of Health, Bethesda, MD, USA).

Cytosolic and nuclear protein extraction

RAW264.7 cells were cultured in 60-mm cell culture dishes for 24 h and pretreated with PJRE (0–100 μg/mL). After 1 h, cells were stimulated with LPS (1 μg/mL) for 30 min. Nuclear and cytoplasmic proteins were extracted using an NE-PER Nuclear and Cytoplasmic Extraction Kit (Thermo Fisher Scientific) according to the manufacturer's instructions.

Immunofluorescence staining

RAW264.7 cells were cultured in 4-well cell culture slides for 24 h and pretreated with PJRE (0–100 μg/mL). After 1 h, cells were stimulated with LPS (1 μg/mL) for 24 h. The cells were then fixed in 4% paraformaldehyde for 1 h and washed thrice with PBS. The cells were cultured in 1% bovine serum albumin (BSA) for 1 h and incubated overnight at 4°C. The cells were washed twice with PBS and incubated with Alexa Fluor 488-conjugated goat anti-mouse IgG antibody in 1% BSA for 1 h at room temperature. The cells were then washed three times with PBS and mounted with DAPI. Images were obtained using a fluorescence microscope (Carl Zeiss; Oberkochen, Germany).

Statistical analysis

Results are presented as the mean ± SD. Statistical analyses were conducted using GraphPad Prism 10 software (GraphPad Software, Inc., La Jolla, CA, USA). The significance of differences between groups was determined using one-way analysis of variance (ANOVA), followed by Tukey's post hoc test. $P < 0.05$ was considered statistically significant.

Results

Concentrations of the major components in Peucedanum japonicum samples

Roots of *P. japonicum* harvested from the farms were dried and extracted using ethanol. The ethanol extract and standard compounds were prepared at concentrations of 1 and 5 mg/mL, respectively. To identify the main components of the roots of *P. japonicum*, the retention times of the ethanol extract and standard compounds were compared to identify the main components of the *P. japonicum* roots. As shown in Figure 1C, six main signals were detected in the ethanol extract. The signals (**1**–**6**) were identified as 3′-acetyl-4′-*O*-senecioylkhellactone

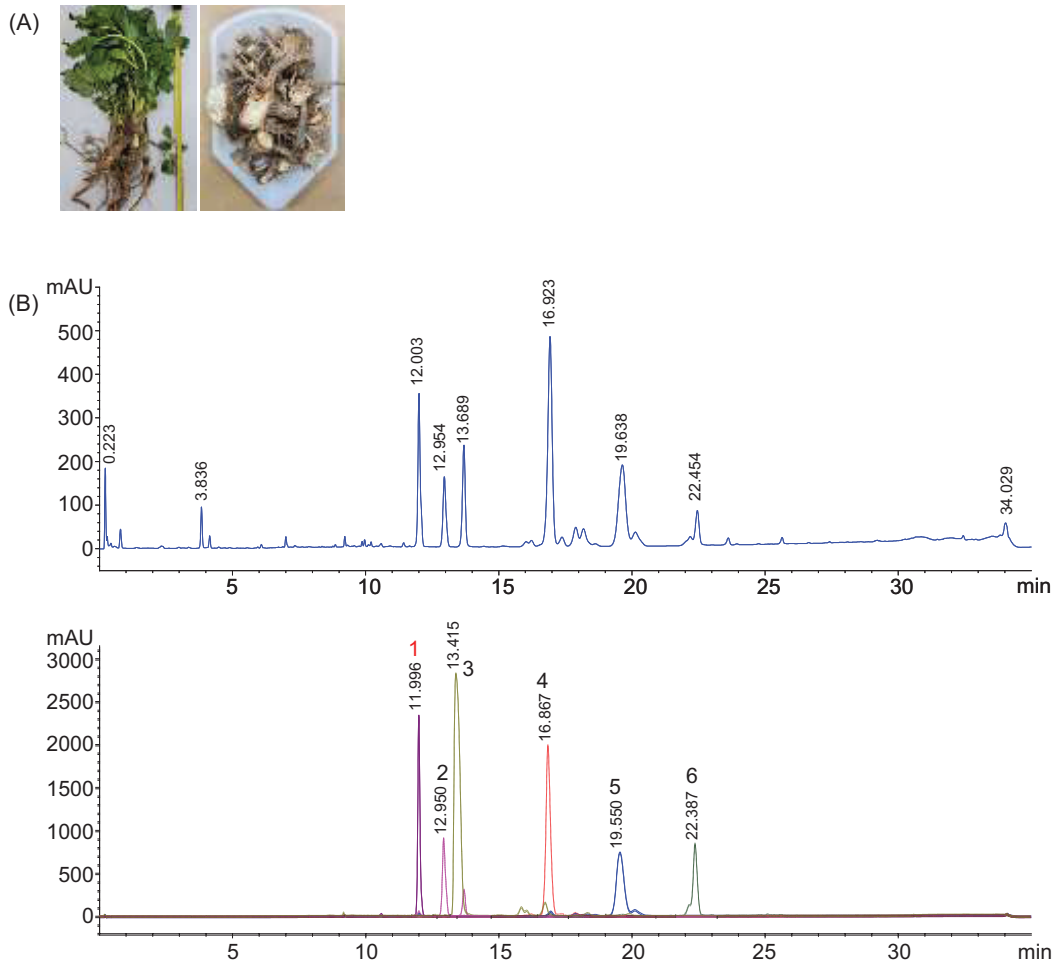

Figure 1 UHPLC profile of the chemical constitutes of *Peucedanum japonicum* roots. Harvested *Peucedanum japonicum* and its dried roots (A). The signals of the ethanol extract *Peucedanum japonicum* roots and standard compounds (**1**, 3′-acetyl-4′-*O*-senecioylkhellactone; **2**, 3′-acetoxy-4′-(2-methylbutyroyl) khellactone; **3**, falcarindiol; **4**, 3′,4′,-disencioylkhellactone; **5**, 3′-sensecioyl-4′-isovalerylkhellactone; **6**, 3′-isovaleryl-4′-[2-methylbutyroyl] khellactone) (B).

(12.0 min), 3′-acetoxy-4′-(2-methylbutyroyl) khellactone (12.9 min), falcarindiol (13.6 min), 3′,4′,-disencioylkhellactone (16.8 min), 3′-sensecioyl-4′-isovalerylkhellactone (19.6 min), 3′-isovaleryl-4′-[2-methylbutyroyl] khellactone) (22.4 min), (Figures S1-S6).

Suppressive effect of PJRE on C48/80-induced atopic dermatitis-like skin symptoms in mice

Previously, we reported that *P. japonicum* Thunberg leaf extract (PJLE) exhibited potent anti-inflammatory properties in RAW 264.7, but we did not examine its effects on AD-like skin symptoms.[19] In this study, we examined whether PJRE could alleviate AD-like skin symptoms by monitoring the scratching behavior in mice. Briefly, mice were subcutaneously injected with C48/80 between both shoulders to induce itching after PJRE administration. Although scratching behavior increased rapidly in mice treated with vehicle, the number of scratching behaviors decreased significantly in mice treated with PJRE (Figure 2B).

Next, we evaluated the histological changes in the mouse skin tissue. Inflammatory cell infiltration and mast cell degranulation were increased in mice treated with vehicle, and both were suppressed in mice treated with PJRE (Figures 2C and 2D).

Suppressive effect of PJRE against mast cell activation in PMA/A23187-induced HMC-1 cells

We treated HMC-1 cells with PJRE for 24 h and evaluated their effects on cell viability using the MTT assay. The results confirmed that PJRE was not cytotoxic to HMC-1 cells at concentrations of up to 100 μg/mL (Figure 3A). As AD symptoms caused by C48/80 are associated with increased mast cell activation, we investigated the effects of PJRE on HMC-1 cell activation. We measured the secretion of histamine and IL-31, which are factors that cause itching, and the production of inflammatory cytokines. The levels of histamine and IL-31 secretion were reduced and the production of TNF-α, IL-6, and IL-8 was suppressed by PJRE treatment (Figures 3B and 3C). In addition, these inflammatory cytokines were regulated by the transcription factor NF-κB, and we confirmed that PJRE treatment suppressed NF-κB activation (Figure 3D).

These observations indicate that PJRE suppressed AD-like skin symptoms, such as reduced scratching behavior

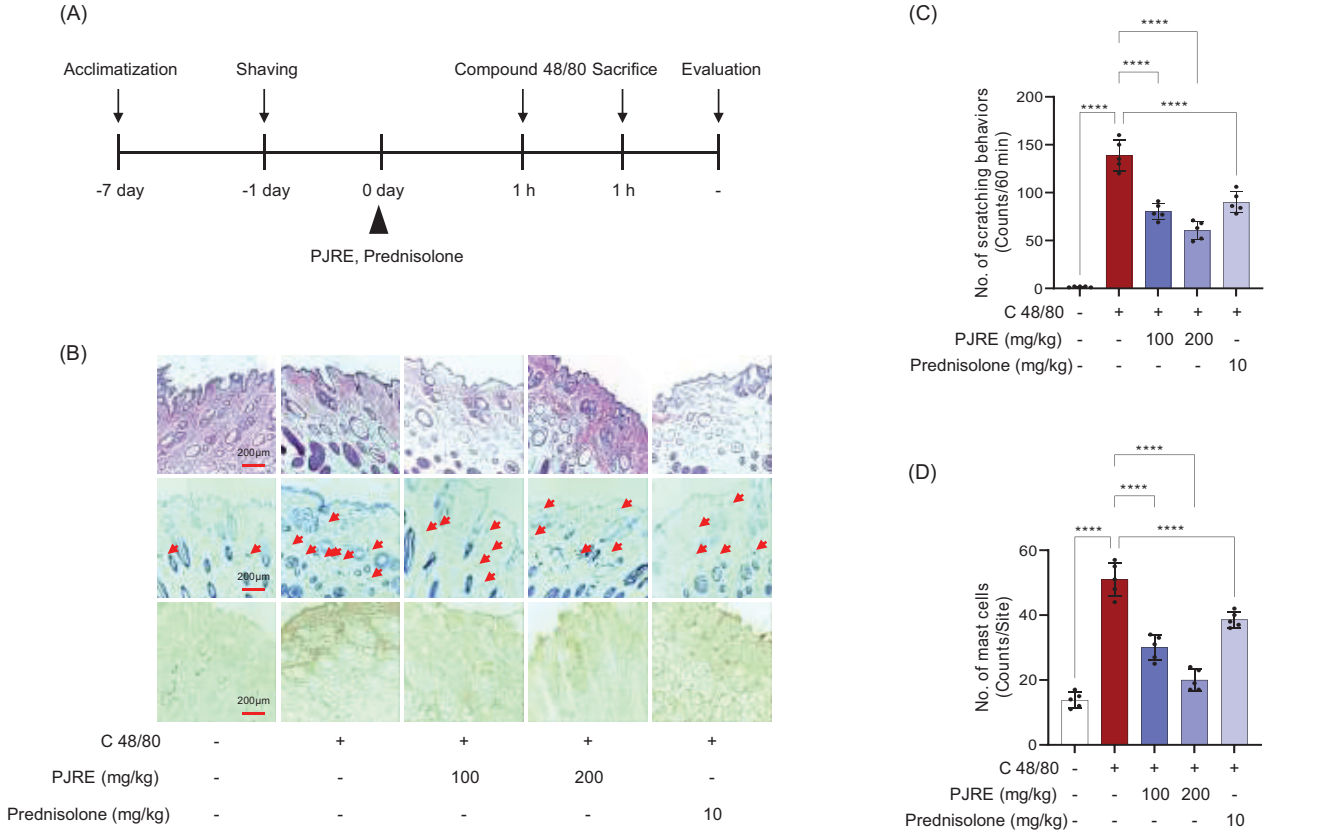

Figure 2 Inhibitory effect of PJRE on scratching behavior in C48/80-stimulated AD-like skin lesions in mice. (A) Experimental design for AD-like lesions induction and treatment method. (B) Scratching behavior. (C) Histological changes. Morphological changes of skin stained with hematoxylin/eosin; Mast cell degranulation of skin stained with toluidine blue; Immunohistohemically stained tissues showing tryptase, a marker of mast cell degranulation. (D) The number of mast cells. Images were taken at 10X magnification. Results are means ± SD (N = 5). Different small case letters indicate significant differences at $P < 0.05$. AD: Atopic dermatitis (AD); PJRE: *Peucedanum japonicum* Thunberg root extract; SD: Standard deviation.

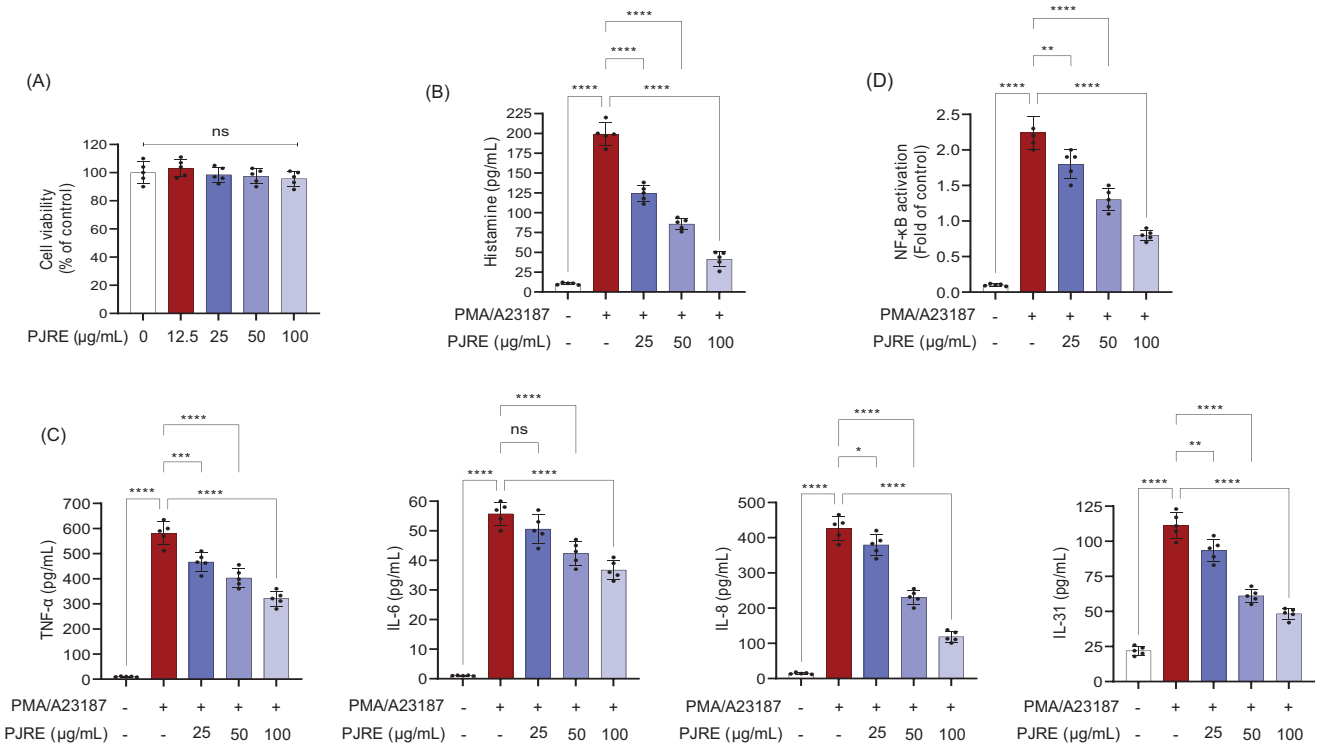

Figure 3 Inhibitory effect of PJRE on pruritus mediators and NF-κB activation in PMA plus A23187-stimulated HMC-1 cells. (A) Cytotoxicity effect of PJRE on HMC-1 cells. (B) Suppressive effects of PJRE on histamine production. (C) Suppressive effects of PJRE on pruritus cytokines. (D) Suppressive effects of PJRE on NF-κB activation. Results are means ± SD (N = 3). Different small case letters indicate significant differences at $P < 0.05$. NF-κB: Nuclear factor-kappa B; PMA: Phorbol 12-myristate 13-acetate.

and secretion of histamine, interleukins, and inflammatory cytokines, by preventing mast cell activation.

Suppressive effects of PJRE on inflammation in LPS-stimulated Raw 264.7 cells

In a previous study, we demonstrated the strong anti-inflammatory effects of PJLE in Raw 264.7.[19] Next, we evaluated the anti-inflammatory effects of PJRE in Raw 264.7 cells. First, we treated Raw 264.7 cells with PJRE for 24 h to examine its effects on cell viability using the MTT assay. The results confirmed that PJRE had no cytotoxic effects against Raw 264.7 cells at concentrations of up to 100 μg/mL (Figure 4A). Next, we evaluated the anti-inflammatory effects of PJRE against nitric oxide (NO) production as an inflammatory factor. The LPS-induced NO production was decreased by PJRE treatment in a concentration-dependent manner (Figure 4A). Subsequently, we evaluated the expression of iNOS, COX-2, and other inflammatory cytokines associated with LPS-induced inflammation. As shown in Figure 4B, the expression of iNOS and COX-2, and the production of TNF-α, IL-1β, IL-6, and PGE_2 were significantly reduced by PJRE treatment in a concentration-dependent manner (Figure 4C), (Figure S7A). As these inflammatory cytokines are regulated by NF-κB, we confirmed that the phosphorylation and immunofluorescence of NF-κB were suppressed by PJRE treatment (Figure 4D and Figure S7B). In addition, we evaluated the upstream signaling pathways responsible for the anti-inflammatory effects of PJRE in Raw 264.7 cells. PJRE treatment decreased the LPS-induced phosphorylation of Akt, ERK1/2, and p38 MAPK in a concentration-dependent manner (Figure 4E and Figure S7C).

Effects of PJRE on antioxidant activity in LPS-stimulated Raw 264.7 cells

HO-1 is a representative antioxidant enzyme that plays an important role in regulating LPS-induced inflammation in Raw 264.7 cells.[19] Previously, we showed that PJLE exerts antioxidant and anti-inflammatory effects in Raw 264.7 cells.[19] In this study, we evaluated the effects of PJRE on antioxidant enzymes in Raw 264.7 cells. The LPS-induced HO-1 expression was significantly increased by PJRE treatment in a concentration-dependent manner (Figure 4F and Figure S7D). Because HO-1 gene expression is regulated by the transcription factor NRF2, we confirmed that NRF2 nuclear translocation was increased by PJRE treatment (Figure 4F and Figure S7D). To confirm the contribution of PJRE to the inhibition of NO production, we evaluated NO production in the presence of the HO-1 inhibitor SnPP in Raw 264.7 cells. LPS-induced NO production was significantly reduced by PJRE treatment. However, SnPP neutralized the inhibitory effect of PJRE on LPS-induced NO production (Figure 4G).

These observations indicate that PJRE suppressed the inflammatory response, including reducing the levels of

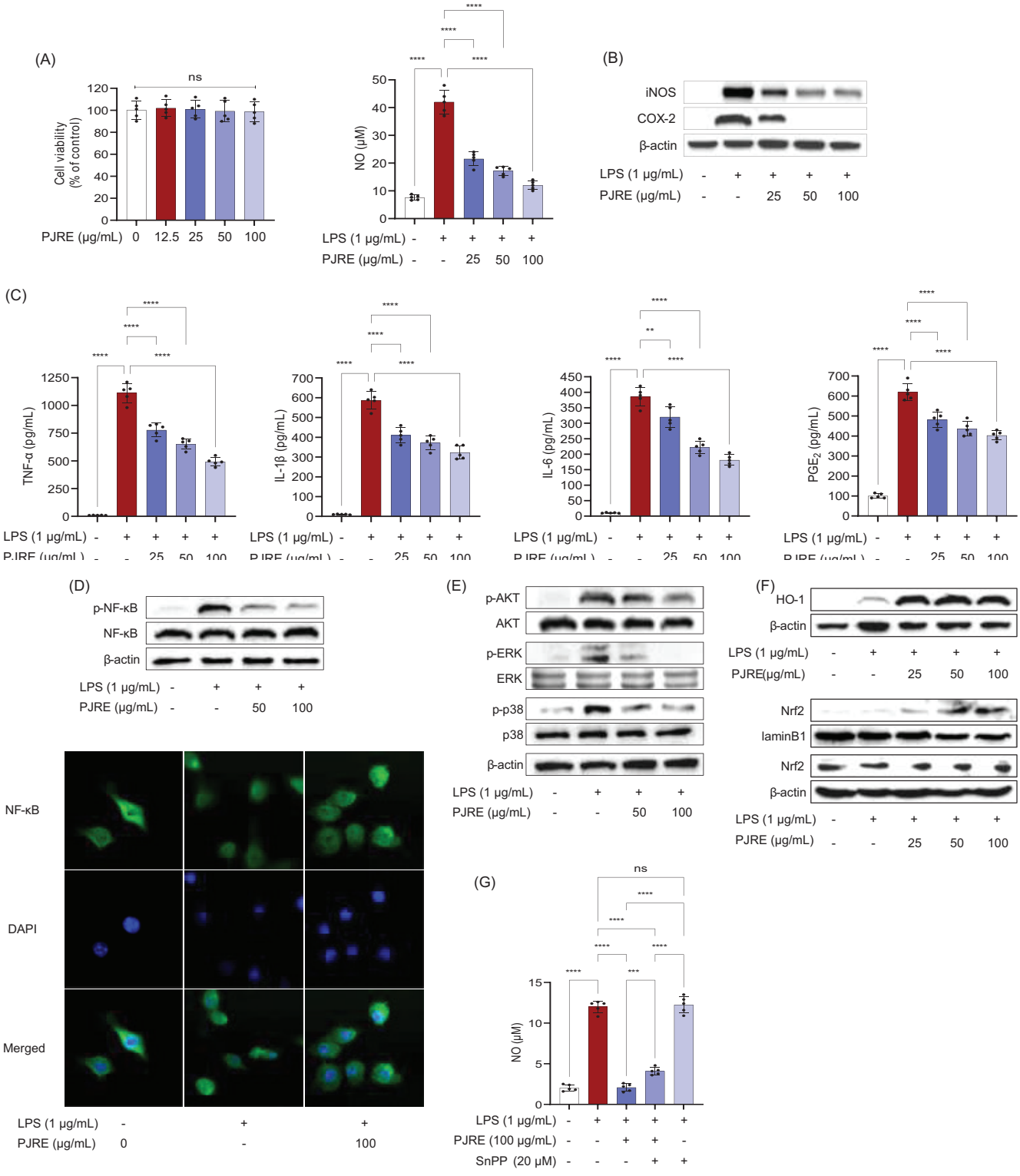

Figure 4 Inhibitory effect of PJRE on inflammation in LPS-induced RAW264.7 cells. (A) Effect of PJRE on cytotoxicity and NO production. (B) Suppressive effects of PJRE on iNOS and COX-2 expression and cytokines secretion. (C) Suppressive effects of PJRE on transcription factor NF-κB activation. (D) Suppressive effects of PJRE on the phosphorylation of Akt, ERK1/2, and p38 MAPK. (E) Suppressive effects of PJRE on the Nrf2-mediated HO-1 activation. Results are means ± SD (N = 3). Different small case letters indicate significant differences at $P < 0.05$. COX-2: Cyclooxygenase-2; HO-1: Heme oxygenase-1; iNOS: Inducible nitric oxide synthase; LPS: Lipopolysaccharide; NO: Nitric oxide; Nrf2: Nuclear factor-erythroid 2 related factor 2.

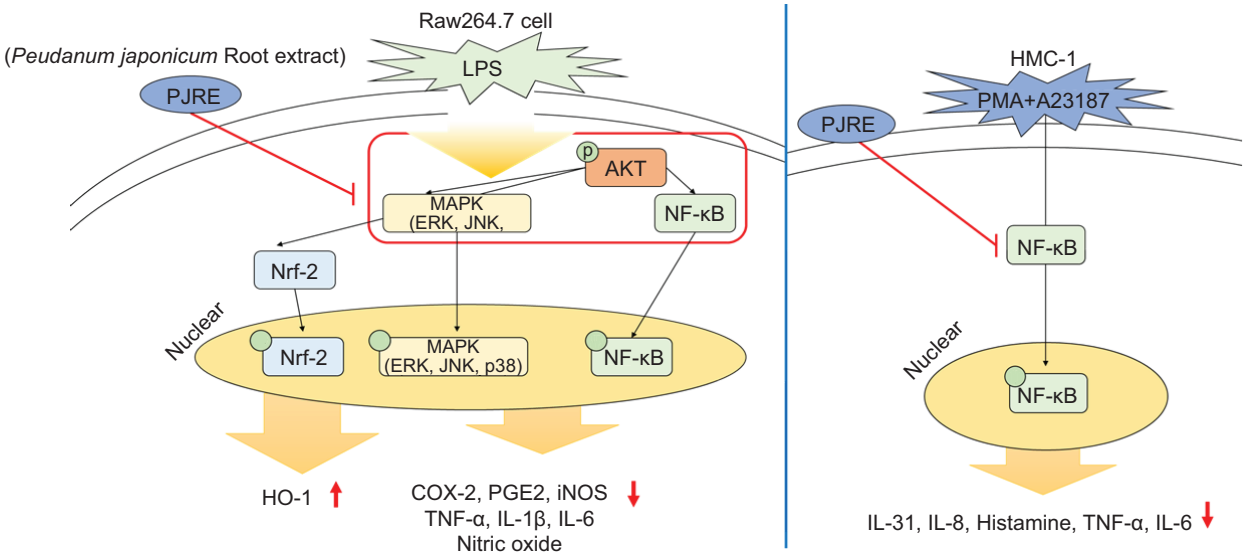

Figure 5 Schematic diagram of possible anti-inflammatory mechanism of PJRE.

NO production, iNOS and COX-2 expression, and inflammatory cytokines, by inhibiting NF-κB and MAPK and inducing antioxidant enzyme production (Figure 5).

Discussion

AD-like skin disease is an inflammatory disease characterized by chronic inflammation and immunomodulatory disorders. The prevalence of AD and its impact on global health are increasing and there is a need to develop novel treatments to improve its symptoms.[19] Nonsteroidal anti-inflammatory drugs, corticosteroids, immunosuppressants, and biological drugs have been used to treat AD-like skin symptoms.[19] However, these drugs have limited efficacy and various side effects. Therefore, alternative treatments are required.[19] Various plant extracts have been used for centuries as folk remedies for improving AD-like skin symptoms in Asia. The leaves and roots of *P. japonicum* Thunberg have long been used in Korea for the treatment of colds, coughs, and headaches, and have been used in oriental medicine to treat stroke. Recently, *P. japonicum* Thunberg has attracted attention as a functional food because it has been reported to have anticancer effects and improve the symptoms of rheumatoid arthritis.[19] However, the effect of PJRE in relieving skin itchiness has not yet been reported. Therefore, we examined the use of PJRE to relieve skin itching, especially AD-like skin symptoms, and investigated its effects and related signaling pathways in animal and cellular models. Identification of the components of plant extracts with low toxicity involved in the improvement of AD-like skin symptoms and anti-inflammatory effects is important for the development and clinical application of effective drugs. In this study, we screened a chemical library using an Agilent 1290 Infinity II system with a diode array detector to identify the components of PJRE responsible for its effects on AD-like skin symptoms, mast cell activation, inflammation, and antioxidant induction.

Table 1 UHPLC profile of the components in *Peucedanum japonicum*.

S.No	Time	Component
1	12.0min	3′-acetyl-4′-*O*-senecioylkhellactone
2	12.9min	3′-acetoxy-4′-(2-methylbutyroyl) khellactone
3	13.6min	falcarindiol
4	16.8min	3′,4′,-disencioylkhellactone
5	19.6min	3′-sensecioyl-4′-isovalerylkhellactone
6	22.4min	3′-isovaleryl-4′-(2-methylbutyroyl) khellactone

Ultra-high-performance liquid chromatography (UHPLC).

AD-like symptoms including dry skin, itching, scratching, and erythema are caused by exposure to various allergens.[19] The main characteristics of AD-like skin lesions are itching and scratching, both of which result in a reduced quality of life.[19] AD-like lesions are characterized by increased skin thickness owing to mast cells.[19] In addition to the increase in mast cells in the dermis, the pathological characteristics of AD-like skin lesions include epidermal thickening, lymphocyte infiltration, and dermal fibrosis. We applied C48/80 to the mouse skin to induce pruritus in a mouse model. In this study, skin scratching due to mast cell infiltration was increased by C48/80 was reduced by PJRE in a concentration-dependent manner. We confirmed that the reduction in skin pruritus caused by PJRE was comparable to the effect of prednisolone, a topical steroid, as a positive control. In addition, because the onset of AD-like skin symptoms is closely related to mast cell activation, we evaluated the inhibitory effects of PJRE on the activation of HMC-1 cells in a human mast cell model. The ELISA results confirmed that the levels of inflammatory cytokines and histamine secretion induced by PMA and A23187 were decreased by PJRE in a concentration-dependent manner.

To further evaluate the effect and mechanism of action of LPS on the skin inflammatory response, we investigated the LPS-induced inflammatory response in mouse macrophages. Previously, we reported that PJLE exhibited strong anti-inflammatory effects against LPS-induced mouse macrophages. In this study, we evaluated the anti-inflammatory effects of PJRE in LPS-induced mouse macrophages. Our results confirmed that, in addition to PJLE, PJRE also exhibits its strong anti-inflammatory effects by inhibiting the phosphorylation of NF-κB as an inflammatory transcriptional regulator.

Atopic dermatitis (AD)-like skin models are usually sensitized and induced by combining specific antigens (e.g., house dust mites and ovalbumin) with adjuvants. Animal models of AD-like skin often mimic chronic models, with elevated serum IgE levels and a Th2-dominant immune response characterized by pruritus, eczematous lesions, and skin thickening.[21] However, chemical-induced models may not fully replicate these immune system characteristics, and may focus primarily on local inflammation and barrier dysfunction. In particular, models that use chemical antigens such as 2,4-dinitrochlorbenzene or 48/80 often induce local dermatitis and may not replicate the systemic features of AD-like skin condition.[22,23]

Nevertheless, we suggest that the effects of PJRE on the prevention and treatment of AD-like skin diseases suggest that the positive effects may vary depending on factors such as the dose, route, and time of administration of PJRE in this study. PJRE inhibits mast cell infiltration and scratching behavior in an AD-like skin mouse model. This may be because the secretion of histamine, NF-κB activation, TNF-α, IL-6, IL-8, and IL-31 in HMC-1 cells, a human mast cell line, was reduced in PJRE. The levels of these immune factors might be sufficient to maintain pruritus in animals. Therefore, this basic research may lay path to further study the effects of PJRE on pruritus in AD patients.

Conclusion

Taken together, the results of this study showed that PJRE significantly alleviated AD-like skin symptoms, activation of human mast cells, and the inflammatory response in mouse macrophages. These observations indicate that PJRE has therapeutic potential in the treatment of AD-like skin symptoms and inflammation in the studied animal model.

Acknowledgments

The research presented in this paper was supported by the "Cooperative Research Program for Agriculture Science and Technology Development" (Project No. RS-2022-RD010239) funded by the Rural Development Administration of the Republic of Korea.

Ethics Approval

All procedures performed in studies involving animals were in accordance with the Jeonju University Institutional Animal Care and Use Committee (approval No: jjIACUC-20230602-2022-0502-A1).

Competing Interests

The authors had no relevant financial or nonfinancial interests to disclose.

Authors Contribution

Jang Hoon Kim contributed to the methodology, formal analysis, investigation, writing – original draft preparation, review, and editing of the manuscript, visualization, supervision, project administration and funding acquisition. Kyung-Sook Han was involved in writing – review and editing of the manuscript. Eun Seo Kang and Ji Hyeon Park contributed to the formal analysis and investigation of the study. Byoung Ok Cho contributed to the conceptualization, methodology, formal analysis, data curation, writing – review and editing of the manuscript, study supervision, project administration, and funding acquisition. Jae Ho Choi was involved in the formal analysis, data curation, original draft preparation, review, and editing, and visualization. All authors read and agreed to the published version of the manuscript.

Conflicts of Interest

The authors report no conflicts of interest in this work.

Funding

The research presented in this paper was supported by the "Cooperative Research Program for Agriculture Science and Technology Development" (Project No. RS-2022-RD010239) funded by the Rural Development Administration of the Republic of Korea.

References

1. Hensel P, Saridomichelakis M, Eisenschenk M, Tamamoto-Mochizuki C, Pucheu-Haston C, Santoro D, et al. Update on the role of genetic factors, environmental factors and allergens in canine atopic dermatitis. Vet Dermatol. 2024;35(1):15–24. https://doi.org/10.1111/vde.13210
2. Yang G, Seok JK, Kang HC, Cho YY, Lee HS, Lee JY. Skin barrier abnormalities and immune dysfunction in atopic dermatitis. Int J Mol Sci. 2020;21(8):2867. https://doi.org/10.3390/ijms21082867
3. Chong AC, Visitsunthorn K, Ong PY. Genetic/environmental contributions and immune dysregulation in children with atopic dermatitis. J Asthma Allergy. 2022;15:1681–700. https://doi.org/10.2147/JAA.S293900
4. Kim JE, Kim JS, Cho DH, Park HJ. Molecular mechanisms of cutaneous inflammatory disorder: Atopic dermatitis. Int J Mol Sci. 2016;17(8):1234. https://doi.org/10.3390/ijms17081234
5. Cetinarslan T, Kumper L, Folster-Holst R. The immunological and structural epidermal barrier dysfunction and skin microbiome in atopic dermatitis-an update. Front

Mol Biosci. 2023;10:1159404. https://doi.org/10.3389/fmolb.2023.1159404
6. Li L, Li ZE, Mo YL, Li WY, Li HJ, Yan GH, et al. Molecular and cellular pruritus mechanisms in the host skin. Exp Mol Pathol. 2024;136:104889. https://doi.org/10.1016/j.yexmp.2024.104889
7. Humeau M, Boniface K, Bodet C. Cytokine-mediated crosstalk between keratinocytes and T cells in atopic dermatitis. Front Immunol. 2022;13:801579. https://doi.org/10.3389/fimmu.2022.801579
8. Aschoff R, Lang A, Koch E. Effects of intermittent treatment with topical corticosteroids and calcineurin inhibitors on epidermal and dermal thickness using optical coherence tomography and ultrasound. Skin Pharmacol Physiol. 2022;35(1):41–50. https://doi.org/10.1159/000518214
9. Drucker AM, Morra DE, Prieto-Merino D, Ellis AG, Yiu ZZN, Rochwerg B, et al. Systemic immunomodulatory treatments for atopic dermatitis: Update of a living systematic review and network meta-analysis. JAMA Dermatol. 2022;158(5):523–32. https://doi.org/10.1001/jamadermatol.2022.0455
10. Drucker AM, Lam M, Prieto-Merino D, Malek R, Ellis AG, Yiu ZZN, et al. Systemic immunomodulatory treatments for atopic dermatitis: Living systematic review and network meta-analysis update. JAMA Dermatol. 2024;160(9):936–44. https://doi.org/10.1001/jamadermatol.2024.2192
11. Filipiuc SI, Neagu AN, Uritu CM, Tamba BI, Filipiuc LE, Tudorancea IM, et al. The skin and natural cannabinoids-topical and transdermal applications. Pharmaceuticals (Basel). 2023;16(7):1049. https://doi.org/10.3390/ph16071049
12. Kwon CY, Lee B, Kim S, Lee J, Park M, Kim N. Effectiveness and safety of herbal medicine for atopic dermatitis: An overview of systematic reviews. Evid Based Complement Alternat Med. 2020;2020:4140692. https://doi.org/10.1155/2020/4140692
13. Chun JM, Lee AR, Kim HS, Lee AY, Gu GJ, Moon BC, et al. *Peucedanum japonicum* extract attenuates allergic airway inflammation by inhibiting Th2 cell activation and production of pro-inflammatory mediators. J Ethnopharmacol. 2018;211:78–88. https://doi.org/10.1016/j.jep.2017.09.006
14. Chun JM, Lee AY, Kim JS, Choi G, Kim SH. Protective effects of *Peucedanum japonicum* extract against osteoarthritis in an animal model using a combined systems approach for compound-target prediction. Nutrients. 2018;10(6):754. https://doi.org/10.3390/nu10060754
15. Kang WS, Choi H, Lee KH, Kim E, Kim KJ, Kim JS, et al. *Peucedanum japonicum* Thunberg and its active components mitigate oxidative stress, inflammation and apoptosis after urban particulate matter-induced ocular surface damage. Antioxidants (Basel). 2021;10(11):1717. https://doi.org/10.3390/antiox10111717
16. Gil TY, Jin BR, Lee JH, An HJ. In vitro and in vivo experimental investigation of anti-inflammatory effects of *Peucedanum japonicum* aqueous extract by suppressing the LPS-induced NF-[Formula: see text]B/MAPK JNK Pathways. Am J Chin Med. 2022;50(8):2153–69. https://doi.org/10.1142/S0192415X22500926
17. Hwang D, Ryu HW, Park JW, Kim JH, Kim DY, Oh JH, et al. Effects of 3'-isovaleryl-4'-senecioylkhellactone from *Peucedanum japonicum* Thunberg on PMA-stimulated inflammatory response in A549 human lung epithelial cells. J Microbiol Biotechnol. 2022;32(1):81–90. https://doi.org/10.4014/jmb.2107.07001
18. Gil TY, Jin BR, An HJ. Peucedanum japonicum Thunberg alleviates atopic dermatitis-like inflammation via STAT/MAPK signaling pathways in vivo and in vitro. Mol Immunol. 2022;144:106–16. https://doi.org/10.1016/j.molimm.2022.02.003
19. Park JH, Kim JH, Shin JY, Kang ES, Cho BO. Anti-inflammatory effects of *Peucedanum japonicum* Thunberg leaves extract in lipopolysaccharide-stimulated RAW264.7 cells. J Ethnopharmacol. 2023;309:116362. https://doi.org/10.1016/j.jep.2023.116362
20. Park JH, Kim JH, Jang SI, Cho BO. Anti-inflammatory of disenecionyl cis-khellactone in LPS-stimulated RAW264.7 cells and the its inhibitory activity on soluble epoxide hydrolase. Heliyon. 2023;9(10):e21032. https://doi.org/10.1016/j.heliyon.2023.e21032
21. Gilhar A, Reich K, Keren A, Kabashima K, Steinhoff M, Paus R. Mouse models of atopic dermatitis: A critical reappraisal. Exp Dermatol. 2021;30(3):319–36. https://doi.org/10.1111/exd.14270
22. Riedl R, Kuhn A, Hupfer Y, Hebecker B, Peltner LK, Jordan PM, et al. Characterization of different inflammatory skin conditions in a mouse model of DNCB-induced atopic dermatitis. Inflammation. 2024;47(2):771–88. https://doi.org/10.1007/s10753-023-01943-x
23. Zheng J, Gu A, Kong L, Lu W, Xia J, Hu H, et al. Cimifugin relieves histamine-independent itch in atopic dermatitis via targeting the CQ receptor MrgprA3. ACS Omega. 2024;9(6):7239–48. https://doi.org/10.1021/acsomega.3c09697

Suppplementry

Table S1 The list of primary antibodies used in western blotting and immunofluorescence experiments. The table includes details such as target protein, catalog number, and source company.

Antibody	Catalog No.	Company
Phospho-Akt (Ser473)	4060	Cell Signaling Technology (Beverly, MA, USA)
Akt	9272	Cell Signaling Technology (Beverly, MA, USA)
Phospho-p44/42 MAPK (Thr202/Tyr204)	9101	Cell Signaling Technology (Beverly, MA, USA)
p44/42 MAPK	9102	Cell Signaling Technology (Beverly, MA, USA)
COX-2 (aa 584-598)	160126	Cayman Chemical (Ann Arbor, MI, USA)
Anti-iNOS/NOS Type II	610328	BD Biosciences (San Diego, CA, USA)
Phospho-p38 MAPK (E-1)	sc-166182	Santa Cruz Biotechnology, INC (Santa Cruz, CA., USA)
p38α MAPK14 (9F12)	sc-81621	Santa Cruz Biotechnology, INC (Santa Cruz, CA., USA)
Phospho-RELA/NFκB p65 (27.Ser 536)	sc-136548	Santa Cruz Biotechnology, INC (Santa Cruz, CA., USA)
RELA/NFκB p65 (F-6)	sc-8008	Santa Cruz Biotechnology, INC (Santa Cruz, CA., USA)
Nrf2 (A-10)	sc-365949	Santa Cruz Biotechnology, INC (Santa Cruz, CA., USA)
Heme Oxygenase 1/HMOX1 (A-3)	sc-136960	Santa Cruz Biotechnology, INC (Santa Cruz, CA., USA)
Lamin B1 (B-10)	sc-374015	Santa Cruz Biotechnology, INC (Santa Cruz, CA., USA)
Actin (C-2)	sc-8432	Santa Cruz Biotechnology, INC (Santa Cruz, CA., USA)

Table S2 The list of secondary antibodies used in western blotting and immunofluorescence experiments. The table includes details such as target protein, catalog number, and source company.

Antibody	Catalog No.	Company
Anti-mouse IgG, HRP-linked	7076	Cell Signaling Technology (Beverly, MA, USA)
Anti-rabbit IgG, HRP-linked	7074	Cell Signaling Technology (Beverly, MA, USA)

Table S3 List of proteins used in ELISA experiments. The table includes details such as target proteins, catalog numbers, and source companies.

ELISA	Species	Catalog No.	Company
TNF-α	Human	DY210	R&D Systems, Inc. (Minneapolis, MN, USA)
IL-6	Human	DY206	R&D Systems, Inc. (Minneapolis, MN, USA)
IL-8	Human	DY208	R&D Systems, Inc. (Minneapolis, MN, USA)
IL-31	Human	DY2824	R&D Systems, Inc. (Minneapolis, MN, USA)
Histamine	Human	ab213975	Abcam (Waltham, MA, USA)
TNF-α	Mouse	DY410	R&D Systems, Inc. (Minneapolis, MN, USA)
IL-1β	Mouse	DY401	R&D Systems, Inc. (Minneapolis, MN, USA)
IL-6	Mouse	DY406	R&D Systems, Inc. (Minneapolis, MN, USA)
PGE_2	Mouse	KGE004B	R&D Systems, Inc. (Minneapolis, MN, USA)

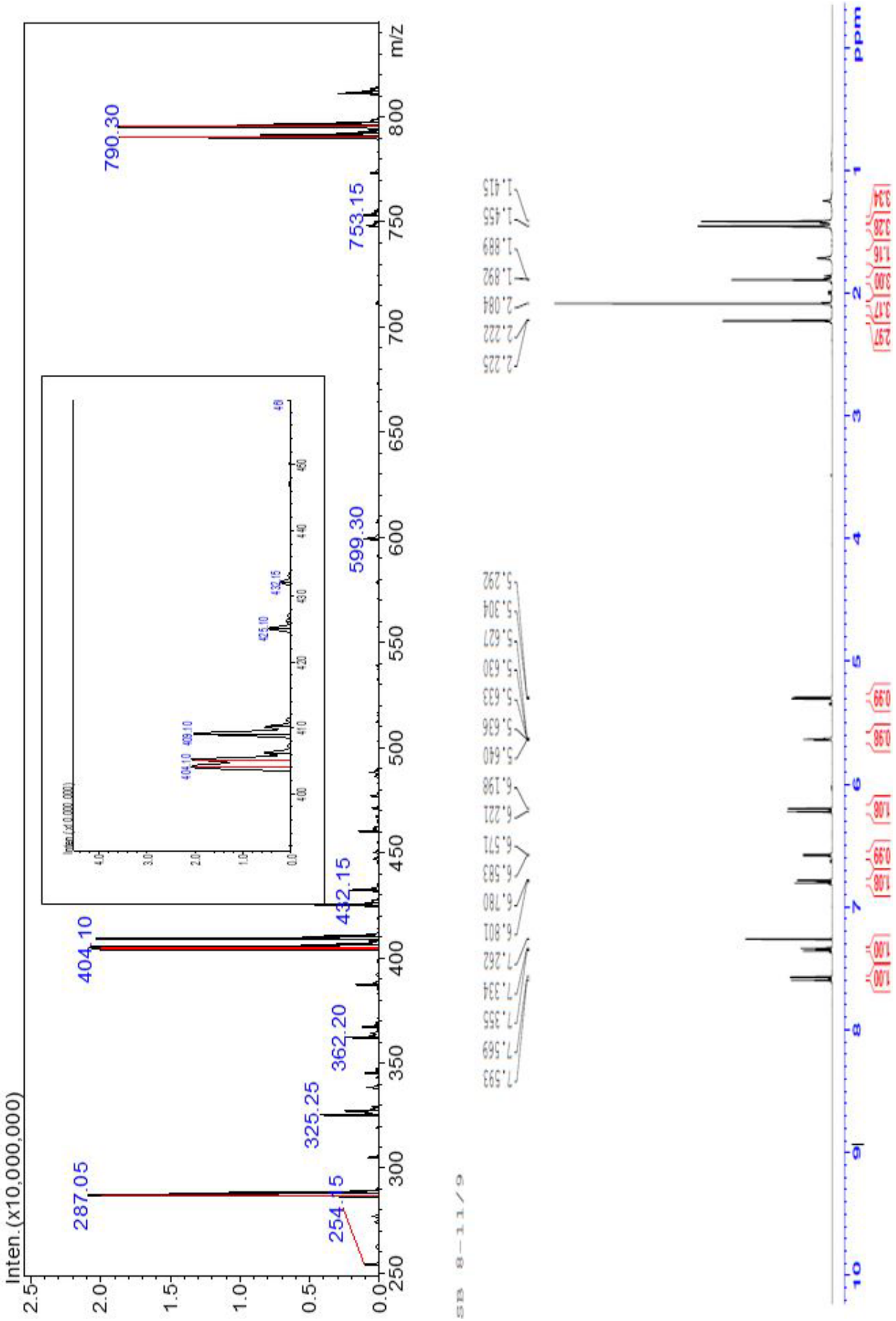

Figure S1 ^{1}H NMR spectrum of 3′-acetyl-4′-*O*-senecioylkhellactone (1) (400 MHz, chloroform-*d*).

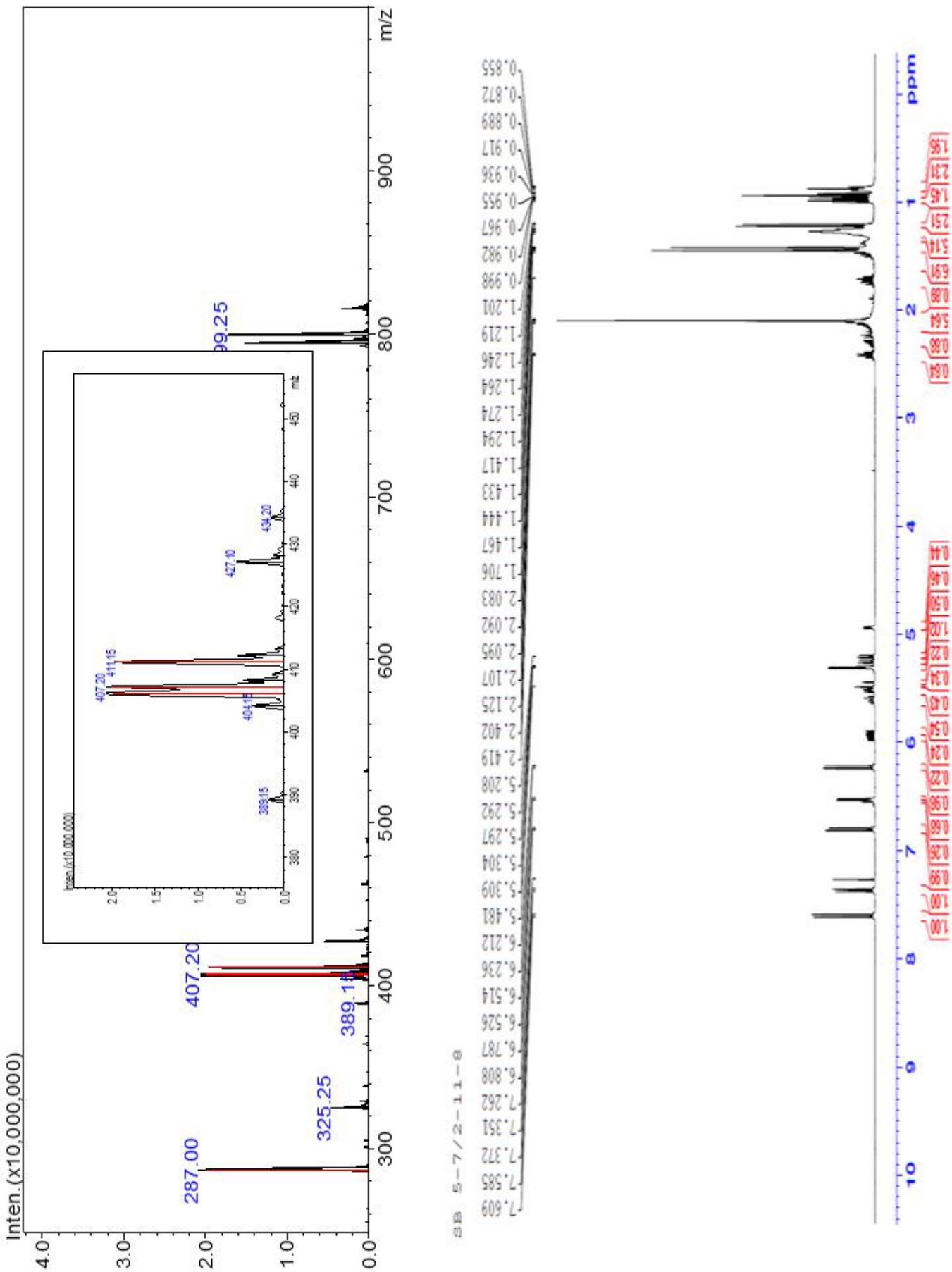

Figure S2 ^{1}H NMR spectrum of 3′-acetoxy-4′-*O*-(2-methylbutyroyl)khellactone (2) (400 MHz, chloroform-*d*).

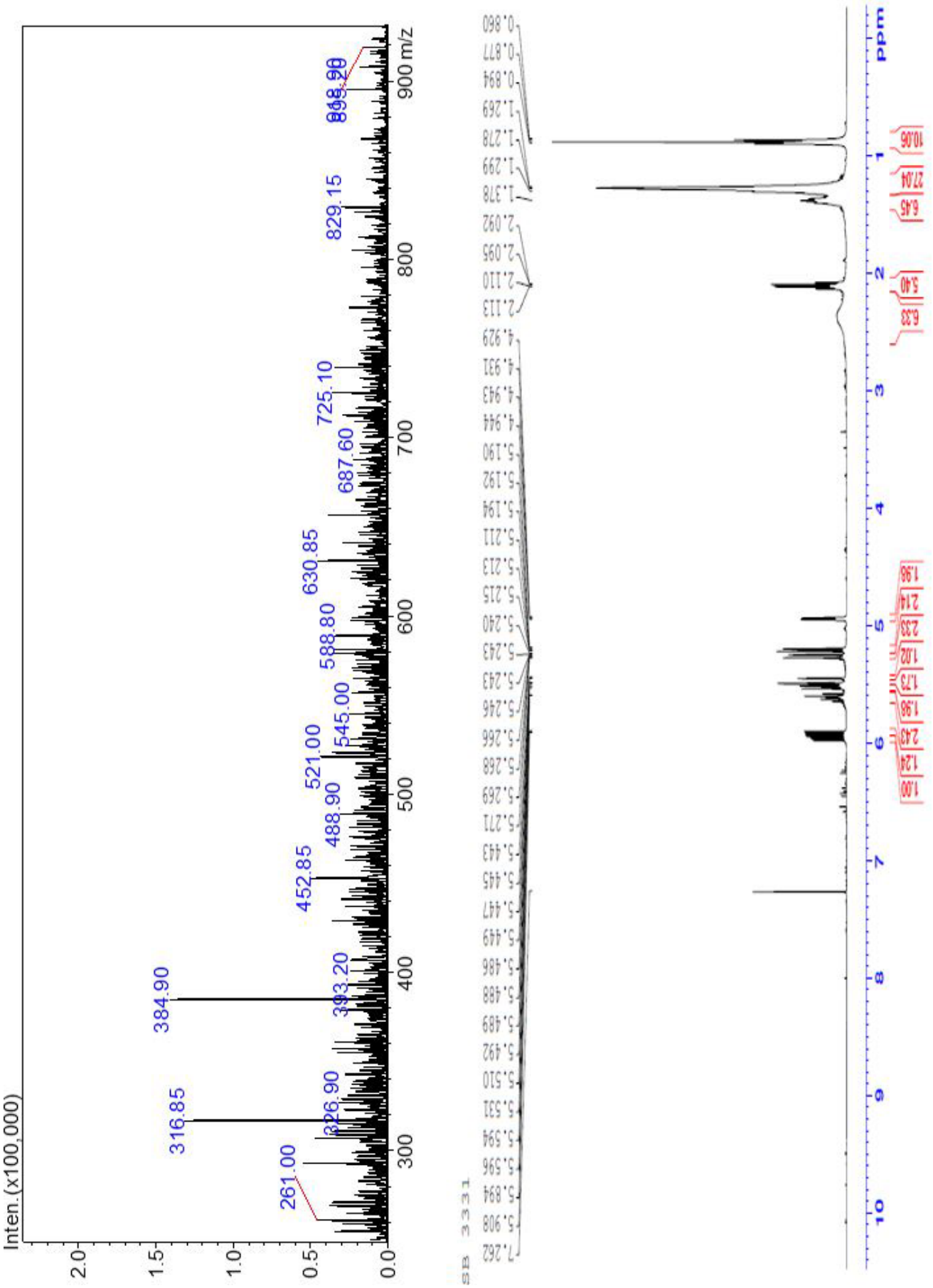

Figure S3 ^{1}H NMR spectrum of farcarindiol (3) (400 MHz, chloroform-*d*).

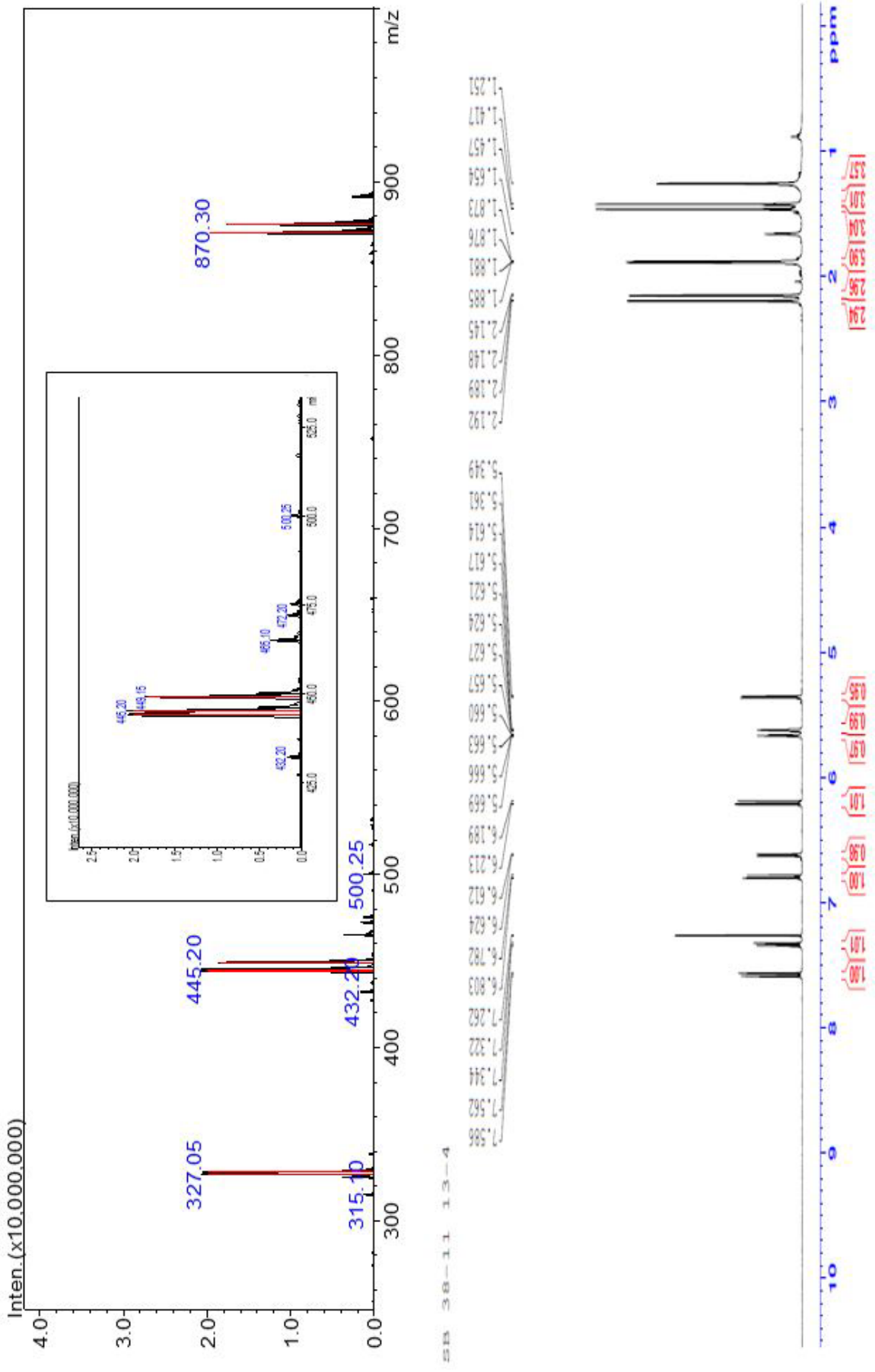

Figure S4 ^{1}H NMR spectrum of 3′, 4′-*O*-disencioylkhellactone (4) (400 MHz, chloroform-*d*).

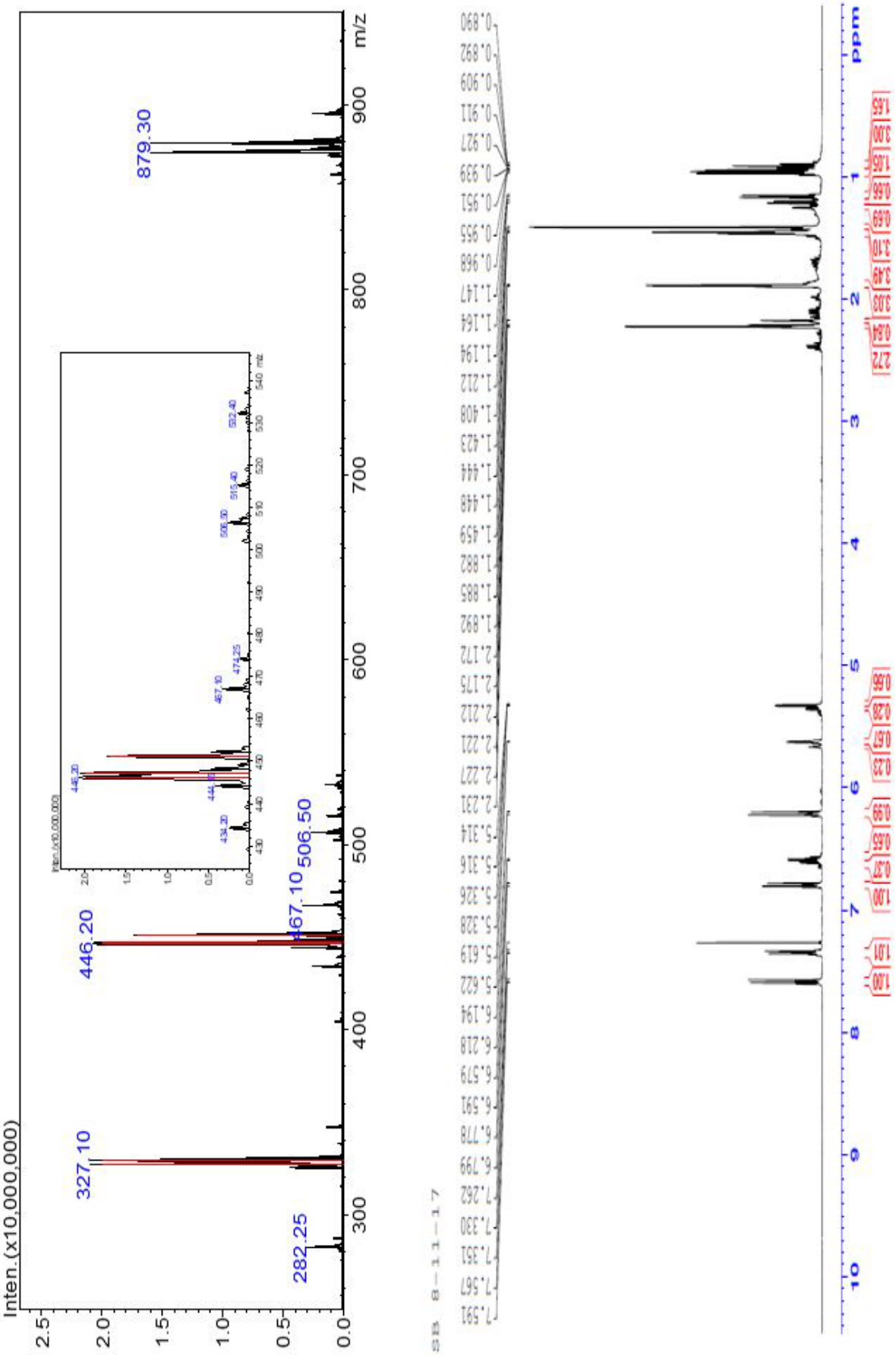

Figure S5 ^{1}H NMR spectrum of 3′-senseciovl-4′-isovalerylkhellactone (5) (400 MHz, chloroform-*d*).

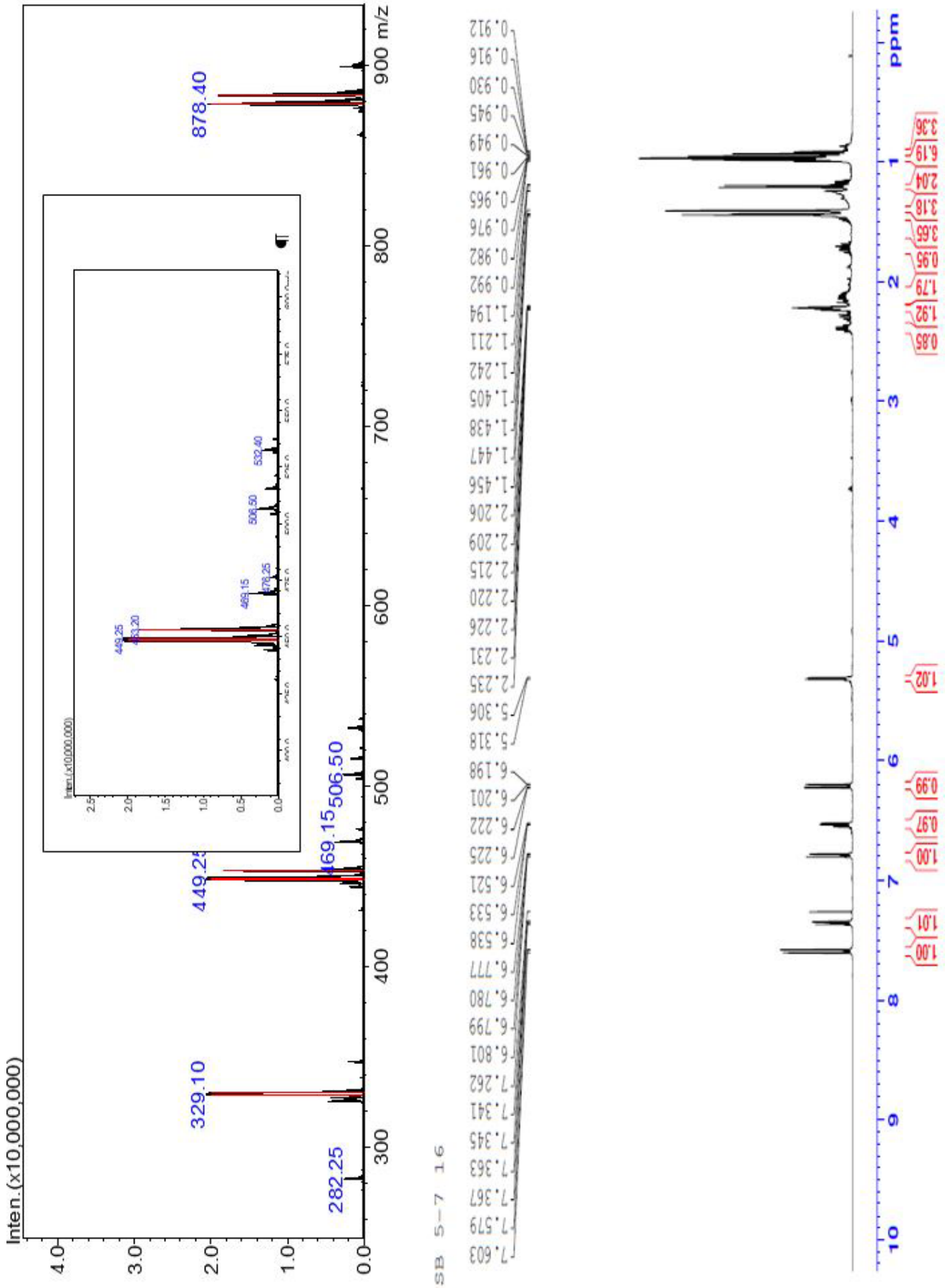

Figure S6 ^{1}H NMR spectrum of 3′-isovaleryl-4′-(2-methylbutyroyl)khellactone (6) (400 MHz, $CDCl_3$-d).

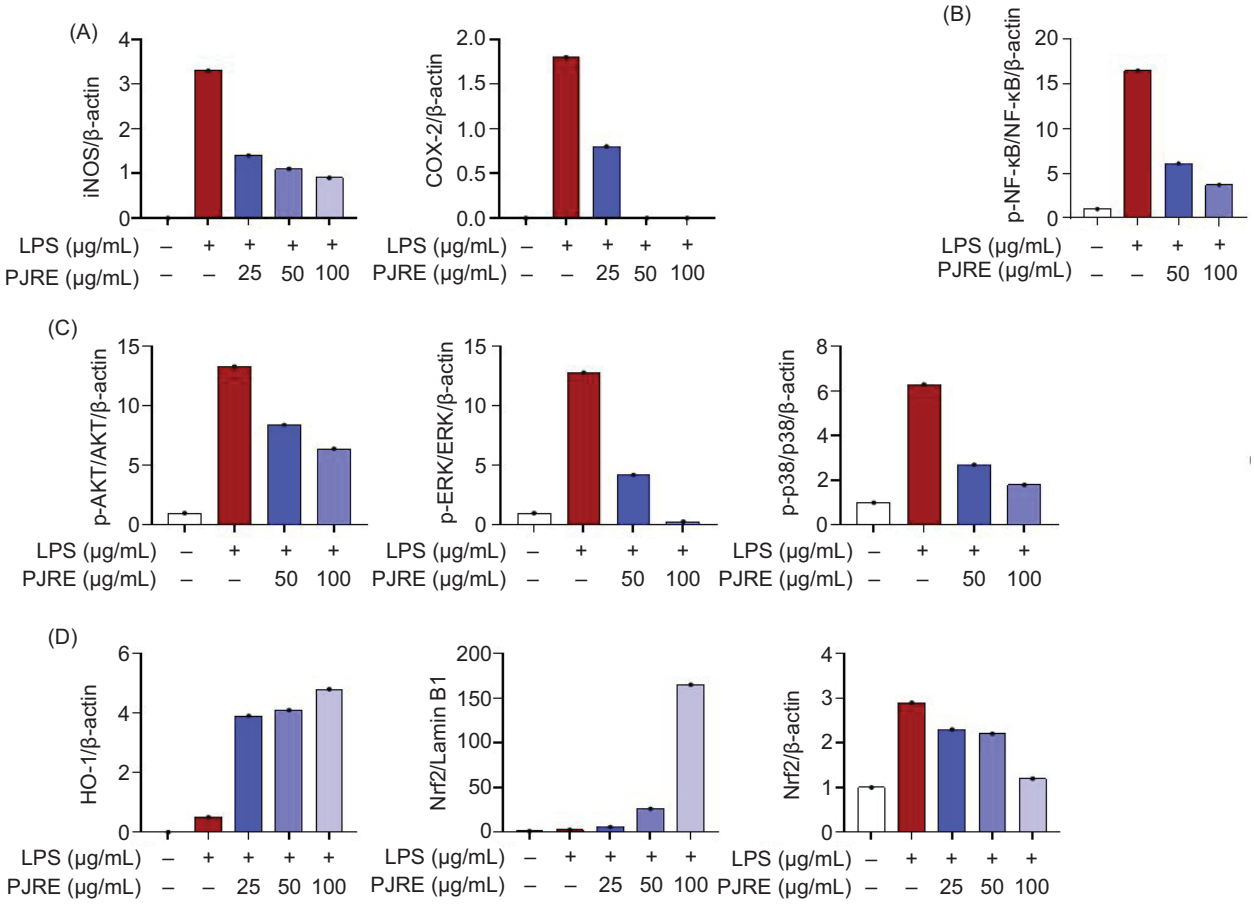

Figure S7 Protein level was analyzed using ImageJ software. Relative expression of the target protein was comparison using β-actin as a control.